

Crack Identification Via User Feedback, Convolutional Neural Networks and Laser Scanners for Tunnel Infrastructures

Eftychios Protopapadakis¹, Konstantinos Makantasis¹, George Kopsiaftis², Nikolaos Doulamis² and Angelos Amditis³

¹Technical University of Crete, Kounoupidiana, 73100, Chania, Greece

²National Technical University of Athens, 9 Iroon Polytechneiou, 15780, Athens, Greece

³Institute of Communication and Computer Systems (ICCS), Zografou 157 80, Athens, Greece

Keywords: Convolutional Neural Networks, User Feedback, Crack Detection, Laser Scanners.

Abstract: In this paper, a deep learning approach synergetically to a laser scanning process are employed for the visual detection and accurate description of concrete defects in tunnels. Analysis is performed over raw RGB images; Convolutional Neural Network serves as the crack detector, during the inspection. In case of a positive detection, the tunnel's cross-section morphology is assessed via 3D point clouds, created by a laser scanner, allowing the identification of deformations in the compartment. The proposed approach, in contrast to the existing ones, emphasizes on applicability (easy initialization, no preprocessing of the input data) and provides a holistic assessment of the structure; reconstructed 3D model allows the fast identification of structural divergence from the original design, alerting the engineers for possible dangers.

1 INTRODUCTION

Nowadays, tunnel inspection, for structural evaluation, is mainly performed through tunnel-wide visual observations by inspectors; a human has to identify structural defects, rate them and then, based on their severity, categorize the liner. Generally, the empirical evaluation can be incomplete mainly due to fatigue, experience, adverse working conditions, or other reasons; it is therefore, unreliable.

Automated approaches for the visual inspection (VI) could deal with most of the aforementioned issues, assuming that they have adequate detection abilities. These methods exploit, mainly, image processing and machine learning techniques. Automated approaches have been applied in various cases including roads, bridges, fatigues, and sewer-pipes (Pynn et al., 1999; Kim and Haas, 2000; Tung et al., 2002; Sinha and Fieguth, 2006).

Current research, in robotics and relevant sectors, presents a variety of sophisticated and reliable components, needed in automated systems. Such components can perform quick and robust inspection/assessment, in general transportation and tunnel infrastructures. However, what is still missing is a holistic approach integrating all these components into a system.

Related work on VI can be divided in two categories: (a) The conventional paradigm and (b) the deep learning approach. In the conventional paradigm, we have to construct complex handcrafted features and, then, train the classifier(s). However, there is a great variety in defect types, making difficult the feature construction/selection task (Halfawy and Hengmeechai, 2014). Deep learning models (Hinton and Salakhutdinov, 2006; Hinton et al., 2006) are a class of machines that can learn a hierarchy of features by building complex, high-level features from low-level ones, automating the process of feature construction for the problem at hand.

The work presented in this paper, involves a VI mechanism using both Convolutional Neural Networks (CNNs) and laser scanners. Such a computer vision scheme is easy to integrate with any robotic part, facilitating the creation of an actual and independent robotic inspector. The CNN is applied for the crack identification, given an RGB image. In case of defect detection, the laser scanner is activated, providing with an detailed 3D model of the investigated cross section.

1.1 Related Work

Intensity features and Support Vector Machines (SVMs) for crack detections on tunnel surfaces were used in (Liu et al., 2002). Color properties, different non-RGB color spaces and various learning algorithms are also investigated in (Son et al., 2012). Edge detection techniques are applied in (Abdel-Qader et al., 2003) for detecting concrete defects. Edge detection (i.e. Sobel and Laplacian operators) and graph based search algorithms are also utilized in (Yu et al., 2007) to extract crack information.

An image mosaic technology for detecting tunnels surface defects was further extended in (Mohanty and Wang, 2012). A pothole detection system (Koch and Brilakis, 2011), based on histogram shape-based thresholding and low level texture features, has been used in asphalt pavement images. A concrete spalling measurement system for post-earthquake safety assessments, using template matching techniques and morphological operations, has been proposed by (German et al., 2012).

Histograms of Oriented Gradient features and SVMs are utilized in the work of (Halfawy and Hengmeechai, 2014), to support automated detection and classification of pipe defects. Shape-based filtering is exploited in the work of (Jahanshahi et al., 2013) for crack detection and quantification. The constructed features are fed as input to ANN or SVM classifiers in order to discriminate crack from non-crack patterns.

The work of (Makantasis et al., 2015) exploit a CNN to hierarchically construct high-level features, describing the defects, and a Multi-Layer Perceptron (MLP) that carries out the defect detection task. Such an approach offers an automated feature extraction, adaptability to the defect type(s), and has no need for special set-up for the image acquisition. Nevertheless, there is a major drawback regarding the applicability in real life scenarios: resources spend for data annotation. Data annotation is a time consuming job that requires a human expert; it is therefore prone to segmentation errors.

The approach of (Makantasis et al., 2015) has been further enriched by (Protopapadakis and Doulamis, 2015); they incorporated a prior, image processing, detection mechanism, facilitating the initialization phase. Such mechanism stands as a simple detector and is only used at the beginning of the inspection. Possible defects are annotated and then validated by an expert; after validating few samples, the required training dataset for the deep learning approach has been formed. From this point onwards, a CNN is trained and, then, utilized for the rest of the inspection process.

Regarding the laser scanning technology, an increasing interest takes place in the last few years, due to the very high density of the acquired data. Monitoring tunnel deformations is a crucial and recent laser scanning application, since it is related to the tunnel stability and safety. A number of studies and papers concerns tunnel geometry inspection.

The work of (Han et al., 2013) proposed the light detection and ranging (LiDAR) technique and the minimum-distance projection (MDP) to collect detailed 3D spatial data in a fast and automatic manner, while avoiding the 3D to 2D profile projection step to reduce the associated uncertainties. (Pejić, 2013) proposed a methodology to optimize the scanning parameters, scans registration, the georeferencing approach and the survey control network design.

(Argüelles-Fraga et al., 2013) tried to incorporate several scanning factors, such as tunnel dimensions, scan density, footprint size, incidence angle and scanner location in scanning circular cross-section tunnels in order to achieve the pre-determined accuracy specifications while minimizing the working time. (Nuttens et al., 2014) used a laser scanner to observe differences of the average radius values during the stabilization phase of a newly built circular train tunnel in Belgium. The results of a systematic monitoring could be valuable to the construction engineers to test and validate the theoretical models. (Monserat and Crosetto, 2008) utilized laser scanner datasets and least square method to match 3D surfaces.

1.2 Our Contribution

Existing approaches suggest favourably towards CNN suitability, for VI processes in tunnels. However, there is no consensus regarding the CNN topology and the input data format. Additionally, a rational approach would be the synergy among different VI approaches in order to mitigate individual drawbacks.

Our work utilizes the same detection mechanism, as in (Protopapadakis and Doulamis, 2015). However, the CNN detector is directly utilized over raw data. Rather than changing the image space, using a low level feature extraction (Makantasis et al., 2015), we directly utilize raw image patches. Doing so preserves the adverse effects from wrong feature selection and simplifies the process; both conceptually and practically.

Also, the usage of a laser scanner results in a holistic approach for the VI. Rather than detecting a crack on a plane, we reconstruct the entire cross section. Such an approach provides further information regarding the status of the infrastructure. The time required for the 3D reconstruction is minimized, since

we reconstruct only the areas with possible defects, rather than the entire infrastructure.

The created 3D point clouds support the engineers' effort for a detailed assessment. At first, recreated cross sections are compared to the original ones, as defined in the construction blueprints. Therefore we are able to prevent deterioration or collapsing, saving human lives. Secondly, the 3D models can be stored for future reference, creating a history log for the infrastructure. This kind of information is crucial to any structural monitoring system and is easily accessible, since the point clouds are using standard formats.

2 PROCESSING CHALLENGES

Ideally, the VI approach should have equivalent abilities to human eye inspection. The process should not be affected by angle and distance from the tunnel surfaces, neither from luminosity conditions. Proximity sensors, advanced navigation, and lighting equipment facilitate the acquisition process but cannot guarantee ideal conditions, nor bypass man made occlusions (e.g. wires).

Yet, even if we achieve ideal conditions, the defect types make the problem increasingly difficult for the detection mechanism. The term "defect" can be interpreted in many ways; deformations, cracks, surface disintegration, and other defects are widely known and commonly appear.

Cracks is a common defect; there are structural failure cracks, random cracks, crazing cracks, shrinkage cracks and map-cracking among many others. Cracks can be described as curved lines of various lengths and widths. Change in texture, width variance and discontinuities are, also expected. They appear, primary, as a result of surface disintegration. In more severe cases, they result as severe errors in construction.

Disintegration of the surface is generally caused by three types of distress: (a) dusting, due to carbonation of the surface by unventilated heaters or by applying water during finishing, (b) ravelling or spalling at joints, when pieces of concrete from the joint edges are dislodged and, (c) breaking of pieces from the surface of the concrete, generally caused by delaminations and blistering.

Other defects include discolouration of the concrete, small voids (bugholes) in the surface of vertical concrete placements, and honeycombing, which is the presence of large voids in concrete. Figure 1 illustrates some of the described defects. Such a variety in defect types hinders the feature extraction process; it

is difficult to construct appropriate descriptors.

Fortunately, aforementioned defects have something in common; crack appearance. Cracks appear in concrete *usually as secondary symptoms of other defects*. As such, the identification of a crack should be the first step, prior to an extensive analysis in the surrounding area, using laser scanners.

3 IMAGE ANALYSIS

CNNs can be used as hierarchical computer vision (CV) schemes, among many other algorithms (e.g. (Doulamis, 2014; Doulamis and Matsatsinis, 2012)), in order to make the recognition process just-in-time, and thus significantly reduce the time and effort needed for visual inspections. Nevertheless, CNN initialization requires a lot of resources and time. A secondary image processing mechanism could save valuable resources (Protopapadakis and Doulamis, 2015).

The detection of defects can be seen as an image segmentation problem, which entails to the classification of each one of the pixels in the image into one of two classes: defects (cracks) class and non-defects class. Such a task requires the description of pixels by a set of highly discriminative features that fuse visual and spatial information. CNN is responsible for the creation of such features.

At first grayscale image patches are created over RGB tunnel's surfaces images. These patches consist the CNN's input. Through a hierarchical construction process, complex, high-level features are created for each patch. These features are fed to a MLP that conducts the classification task. As such, visual and spatial information about a specific pixel, located in the center of each patch, is related to its neighbour pixels.

Concretely, in order to classify a pixel p_{xy} , located at (x, y) point on image plane, we use a square patch of size $s \times s$ centered at pixel p_{xy} . If we denote as l_{xy} the class label of the pixel at location (x, y) and as b_{xy} the patch centered at pixel p_{xy} , then, we can form a dataset $D = \{(b_{xy}, l_{xy})\}$ for $x = 1, 2, \dots, w$ and $y = 1, 2, \dots, h$.

These matrices are fed as input into the CNN. Then, the CNN hierarchically builds complex, high-level features that encode visual and spatial characteristics of pixel p_{xy} . The output of the CNN is sequentially connected with the MLP. Therefore, obtained features are used as input by the MLP classifier, which is responsible for detecting the defects.



Figure 1: Illustration of various concrete defect types in tunnel investigation: (a) map cracking, (b) shrinkage crack, (c) flanking and (d) honeycomb.



Figure 2: Illustration of various images acquired and require further investigation.

3.1 Model Initialization

The crack detection is based solely on the CNN. Yet, in order to facilitate the data set creation, we employ an image processing technique. Such technique exploit: the intensity of pixels and their spatial relations, morphological operations and filtering schemes. Additionally, we perform simple shape analysis on detection results. Such an approach does not require annotated data. Yet, it has low generalization ability and it has to be fine tuned for a specific dataset; there are many parameters in the operators.

The data set creation mechanism needs only a few images, which are easily obtained (usually at first few meters, after the tunnels entrance). If there is photographic material, for the specific infrastructure, from previous examinations, few pictures will be selected at random. After the image gathering is complete, the image annotation process is performed.

Shape properties describe the ratio length to width for the detected edges. Further, we are looking for curves. Regarding intensity, pixels corresponding to cracks are expected to be darker than their neighbouring pixels. Thus, based on cracks characteristics our approach consists of the following steps: (a) Lines enhancing, (b) Noise removal, (c) Straight lines removal, (e) Shape filtering, and (f) Morphological reconstruction.

Line enhancement occurs by comparing the intensity of the specific pixel to its neighbours. Such an approach result in "salt and pepper" noise. The next step focuses on noise removal, exploiting a traditional median filter. Straight lines, is something common, and correspond to man made crafts (e.g. wiring) are located according to Hough transform by thresholding the detected outputs.

Shape filtering using appropriate moments is another crucial step. By locating minimum enclosing circles we are able to exclude symmetrical areas. Finally, we perform a classical morphological operation called "opening by reconstruction". Reconstruction starts from a set of starting pixels and then grows in flood-fill fashion to include complete connected components. A step by step illustration of the image processing approach is shown in fig. 4.

3.2 Deep Learning Defect Recognition

In this section, for the sake of completeness, we briefly describe the notion of CNNs. CNNs apply trainable filters and pooling operations on their input resulting in a hierarchy of increasingly complex features. Convolutional layers consist of a rectangular grid of neurons (filters), each of which takes inputs from rectangular sections of the previous layer.

Each convolution layer is followed by a pooling layer that subsamples block-wise the output of the precedent convolutional layer and produces a scalar output for each block. Formally, if we denote the k -th output of a given convolutional layer as h^k whose filters are determined by the weights W^k and bias b^k then the h^k is obtained as:

$$h_{ij}^k = g((W^k * x)_{ij} + b^k) \quad (1)$$

where x stands for the input of the convolutional layer and indices i and j correspond to the location of the input where the filter is applied. Star symbol (*) stands for the convolution operator and $g(\cdot)$ is a non-linear function. Max pooling layers simply take some $k \times k$ region and output the maximum value in that region.

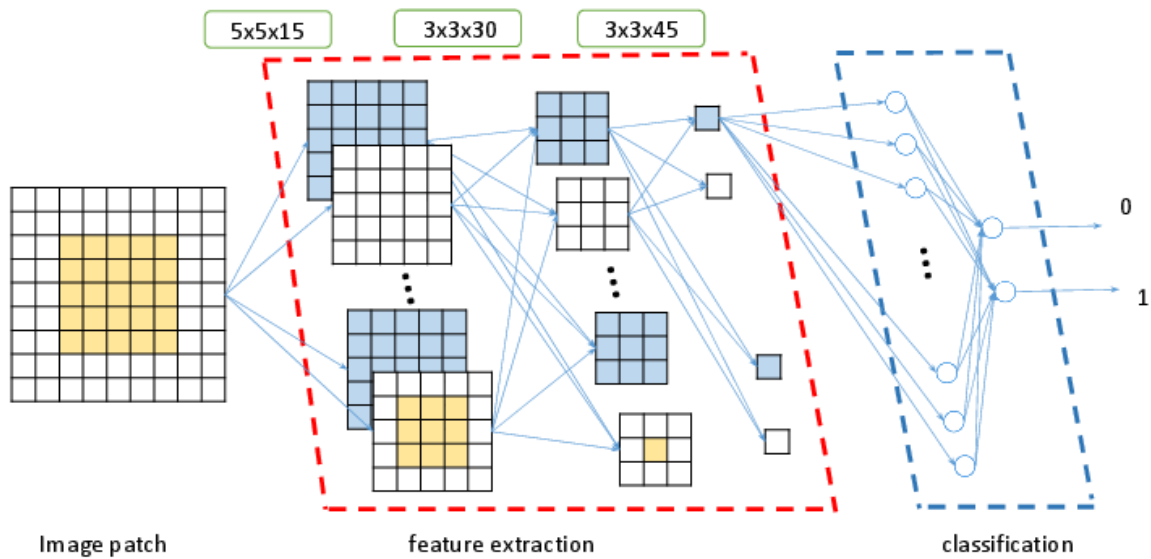


Figure 3: Proposed CNN illustration. Every image patch of size 9×9 is convolved with 15 kernels of size 5×5 at first, then 30 convolution kernels of size 3×3 are used. The final convolution layer uses, also, 45 kernels of size 3×3 .

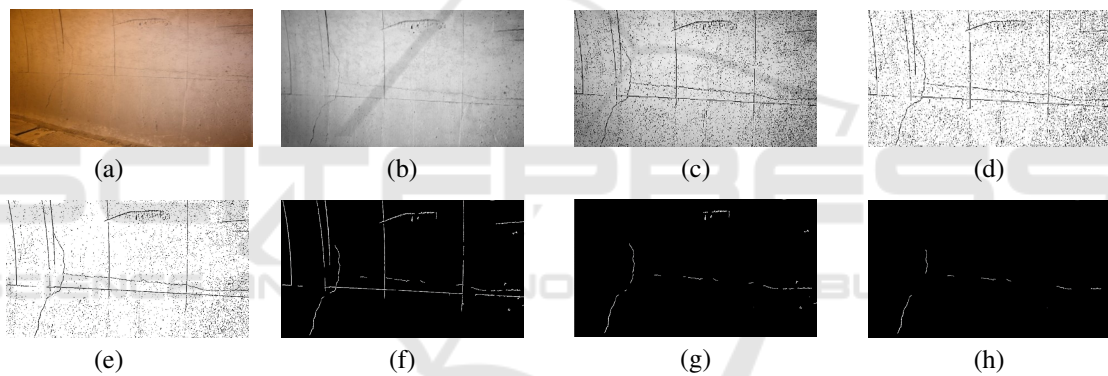


Figure 4: Step by step illustration of the proposed image processing approach; (a) original image, (b) grayscale (c) enhanced lines, (d) binary image, (e) noise removal, (f) area filtered, (g) straight lines removal and (h) final, annotated image.

Max pooling layers introduce scale invariance to the constructed features, which is a very important property for object detection/recognition tasks, where scale variability problems may occur.

However, as pointed in (Makantasis et al., 2015), for the problem of tunnel defects detection, we involve CNNs to construct features that encode spatio-visual information, which indicates the presence or absence of a defect to a specific pixel. Thus, scale invariance, which is addressed through the use of a Gaussian pyramid, does not consist a significant property for our learning model. Due to this fact, we do not involve pooling layers into our CNN architecture.

4 GEOMETRY INSPECTION

The tunnel inspection method presented in the current paper, is performed using not only photogrammetric equipment but also a laser scanner. In general, laser scanners provide a number of useful functionalities for modelling and monitoring tunnels. However, several aspects should be considered while planning the scan of a tunnel to ensure the requirement accuracy and reliability of the measurements, together with a cost effective approach to tunnel surveying:

- Laser scanner specifications: quality and resolution, connectivity options, even portability, in case the device is attached on a moving vehicle (e.g. robotic system).
- Laser scanner accuracy: it is a feature that should

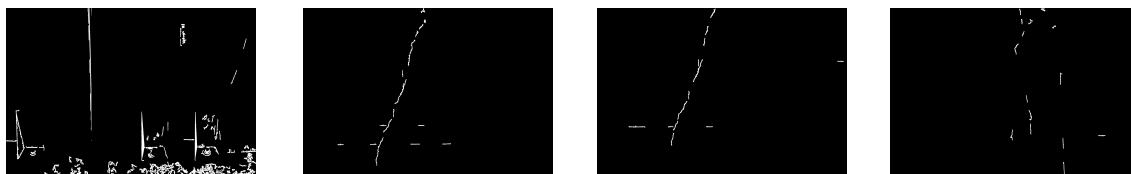


Figure 5: Illustration of crack identification ground truth annotations based on image processing techniques. Such an approach results in many false positive annotations; areas close to the actual cracks are, also, considered as cracks. Areas with significant variation in intensity, texture, or entropy are also faulty classified as cracks.



Figure 6: Illustration of crack identification using CNN. In contrast to the image processing approach, outputs are much refined. The ground truth annotations are limited to the actual cracked regions. A few misclassified pixels may appear at the crack borders.

be considered separately, since it defines the distinctive ability of the scanner and the objects and features of the tunnel surface which can be detected.

- Tunnel dimensions: tunnels total length and width should always be considered in the optimal design of the survey control network.
- Scan time requirements: the relation between resolution/quality and scan duration should be examined, since a time consuming scan could increase exponentially the overall time requirements of the tunnel inspection procedure.

In the current project the FARO® Laser Scanner Focus^{3D} X 130 was used, a mid-range instrument with panoramic architecture, which uses phase shift technology to measure distance. Table 1 contains some significant technical features of the specific laser scanner.

Table 1: FARO Focus^{3D} specifications.

Distance accuracy	up to ± 2 mm
Range	0.6 m up to 130 m
Noise reduction	up to 50%
Field of view	$360^\circ \times 305^\circ$

It is obvious from the absolute values of the distance accuracy, that the Focus^{3D} is not suitable for the detection of small-sized features of the tunnel surface (e.g. cracks). However, the device could be used to detect features which exceed the minimum value of 2 mm, or possible deformations of the tunnel cross section. In the following section a method for the extraction of the tunnel geometry from a point cloud is presented, along with the results from several experimental scans.

4.1 Tunnel Geometry and Point Clouds

In order to derive the geometry of the tunnel cross section, a surface of known equation is presupposed. Usually, the inner surface of a tunnel has a quadratic form, e.g. circle, parabola, or an assembly of circular arcs. In this paper, each scan, i.e. one half of the tunnel cross section, is treated as a part of an elliptic cylinder, which has a cross section of the following form:

$$\frac{x^2}{\alpha^2} + \frac{y^2}{\beta^2} = 1 \quad (2)$$

A nonlinear least-squares solver is utilized to solve the surface fitting problem of the general form

$$\max_x \|f(x)\|_2^2 = \min_x (f_1(x)^2 + f_2(x)^2 + \dots + f_n(x)^2) \quad (3)$$

where x represents the vector of the unknown variables. It should be noted that since the laser scanner is not located at the centre of the elliptic cylinder, the translation and rotation parameters should also be calculated. Therefore, a total number of eight parameters are calculated with the nonlinear least-squares algorithm, including three rotation parameters, three translation parameters and the two parameters of the ellipsis. The trust-region-reflective method (Coleman and Li, 1996; Coleman and Li, 1994) implemented in matlab environment is used as a minimization algorithm.

An initial surface estimation is performed to calculate outliers. Specifically, measured points that are not in close proximity to the surface, based on a user specified threshold, are excluded from the calculations. The parameter value estimation procedure is applied once again, based on the corrected point



Figure 7: Aspect of the experimental tunnel (a) and a rough 3D model (b).

dataset. Features of the tunnel, of considerable size compared to the distinctive ability of the laser scanner, are detected as the discrepancy between the calculated geometric surface and the measured points. Temporal changes in the calculated surface parameters could be used as an indication of tunnel deformations, and provide structural engineers with measuring results regarding the extend of these deformations.

5 SYSTEM EVALUATION

The proposed system was developed on a conventional laptop with quad-core CPU, 8GB RAM, using Theano library (Bastien et al., 2012) in Python. The CNN is compared against the image processing approach, described in sec. 5.1. Compatibility with robotic parts has been also verified using YARP (Fitzpatrick et al., 2008).

All the images originate from Metsovo motorway tunnel in Greece, which is a 3.5km long twin tunnel. In a distance of 20m parallel and north to this bore, runs the ventilation tunnel. The main tunnel suffered a significant deformation due to water inflow. Image data were captured at this part of the tunnel, using a hand held DSLR camera. Figure 2 illustrates various tunnel images during data acquisition process. Regions depicting defects, for each of the captured images, were manually annotated, by experts(i.e. about 100 images).

Proposed approach is applied on the raw image data and its performance is evaluated in regard to the ground truth data. The unbalanced nature of classes would deteriorate the performance of the system; defects span very few areas. As such, we truncate the non-defects class to contain the same number of samples as the class that represents defects. The final dataset that is used for training and testing, is created by concatenating the elements of the two classes.

5.1 Crack Detection using Image Processing Techniques

The image processing technique is similar to the work of (Protopapadakis and Doulamis, 2015). Line enhancement is performed on 13×13 windows by thresholding the 0.99% of the mean intensity value. Then, areas spanning less than 550 pixels are considered noise and, thus, excluded. Hough transform distance and angle resolution were set to 5 pixels and 0 radians respectively. Finally, areas of defects should span at least 30% of the minimum enclosing circle. An indicative result of the annotated images can be found in fig. 5.

5.2 Crack Detection using CNN

The input of the CNN are patches of dimensions $s \times s$. The parameter s determines the number of neighbours of each pixel that will be taken into consideration during classification task. During experimentation process we set the parameter s to be equal to 9, in order to take into consideration the closest 24 neighbours of each pixel.

The value of s can be increased. Yet, an increase in s value results in an increase of computational cost. In our case, setting the parameter s to a value greater than 9, resulted in no further performance's improvement; value of s over 13 resulted in worse classification accuracy.

Having estimate the value s , we can proceed with the CNN architecture design. The first layer of the proposed CNN is a convolutional layer with $C_1 = 15$ trainable filters of dimensions 5×5 . This layer delivers C_1 matrices of dimensions 5×5 (during convolution we do not take into consideration the border of the patch). Due to the fact that we do not employ a max pooling layer, the output of the first convolutional layer is fed to the second convolutional layer (30 kernels of size 3×3). Then, the third layer (45

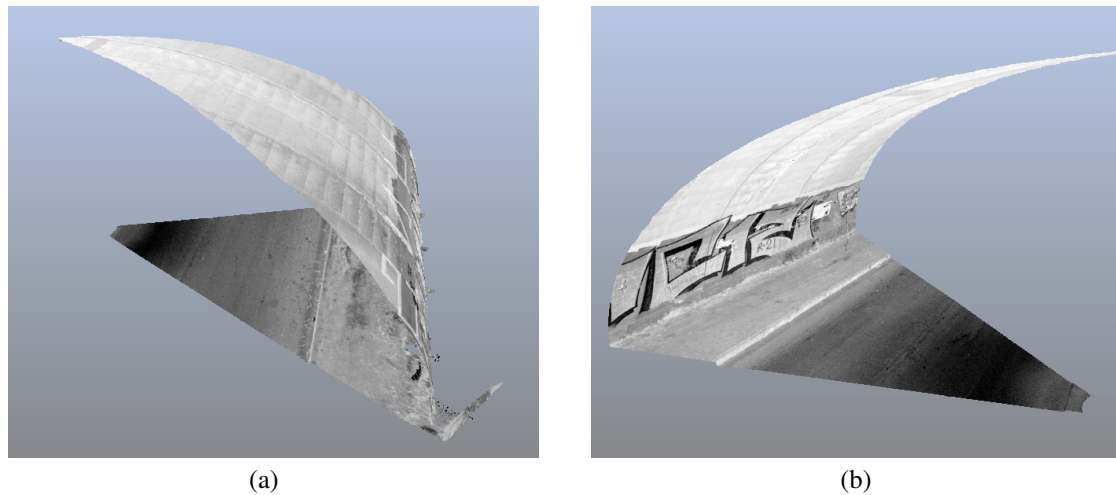


Figure 8: A more detailed 3D model cross section of the inspected tunnel for left (a) and right (b) side respectively.

Table 2: Metrics for quantitative performance evaluation.

Metric	Formula
Sensitivity - (TPR)	$TPR = TP / P$
Specificity - (SPC)	$SPC = TN / N$
Precision - (PPV)	$PPV = TP / (TP + FP)$
Neg. predictive value - (NPV)	$NPV = TN / (TN + FN)$
False pos. rate - (FPR)	$FPR = FP / N$
False discovery rate - (FDR)	$FDR = 1 - PPV$
Miss Rate - (FNR)	$FNR = FN / P$
Accuracy - (ACC)	$ACC = (TP + TN) / (P + N)$
F1 score - (F1)	$F1 = 2 TP / (2 TP + FP + FN)$

kernels of size 3×3) creates the input vectors for the MLP. An indicative result of the annotated images via CNN can be found in fig. 6.

5.3 Performance Evaluation

In this paper we have two possible classes; cracks or non-cracks, named positive (P) and negative (N) class, respectively. Given the outputs, we form the confusion table, which is a 2×2 matrix that reports the number of false positives (FP), false negatives (FN), true positives (TP), and true negatives (TN). Given these values we are able to calculate various performance metrics regarding the defect detection performance.

Calculated metrics formulation is shown in table 2. Metrics of special interest are: Sensitivity (proportional to TP) and miss rate (proportional to FN), which are both strongly connected to crack detection.

5.4 Experimental Scans in Tunnels

The aspects of sec.4 are examined in a relatively small-sized test tunnel, located at the campus of the

National and Kapodistrian University of Athens. The tunnel has a total length of approximately 60 m, and 10 m width. The cross section shape of the tunnel approximates a semicircle, and the texture of the inner surface is characterized by regular rough patterns, due to the construction process. Several rough edges and surfaces which exceed 2 mm, are also present and could be used as surface features to be detected with a laser scanner.

Several scans were performed with different combinations of quality, resolution, vertical and horizontal range. Figure 7 illustrates an aspect of the tunnel, as well as a rough 3D depiction, created by the point cloud. In both scans, in terms of the Focus^{3D} parameters, the resolution was 1/4 and the quality 4x (i.e. 122 kpt/s).

A number of more detailed scans with higher resolution and quality were performed, in order to collect datasets of several tunnel cross sections. Figure 8 presents the results of a cross-sectional scan, with resolution 1/1 and quality 3x (i.e. 244 kpt/s). The vertical scan range was from -62.5° to 90° , while the horizontal range was from 180° to 230° . It should be noted that two independent scans are required to scan a complete cross-section of the tunnel.

6 CONCLUSIONS

In this paper, we point the suitability for deep learning architectures for the tunnel defect inspection problem. The proposed approach employed both a CNN and a laser scanner in a holistic assessment scheme, significantly extending the capabilities of a deep learning approach.

Table 3: Performance evaluation score for both CNN and image processing approaches.

Average scores	ACC	TPR	SPC	NPV	PPV	FNR	FPR	F1
CNN	0.8684	0.8981	0.8387	0.8919	0.8481	0.1019	0.1613	0.8722
Image Processing	0.6337	0.5866	0.6808	0.6284	0.6495	0.4134	0.3192	0.6112

The system evaluates raw images through the CNN detector. In case of a positive identification of a crack the laser scanner is used to provide further details via a method to exploit point clouds, provided by terrestrial scanners.

The proposed method is based on the parametrization of the tunnel surface, using a nonlinear minimization solver and could be employed to detect possible deformations or features of considerable size.

Future work may involve CNN topology optimization schemes, for further performance improvement, or hardware implementation to improve detection times. Additionally, different geometric surfaces can be investigated, in order to achieve better approximation of the inner tunnel surfaces.

ACKNOWLEDGEMENTS

The research leading to these results has received funding from the EC FP7 project ROBO-SPECT (Contract N.611145). Authors wish to thank all partners within the ROBO-SPECT consortium.

REFERENCES

- Abdel-Qader, I., Abudayyeh, O., and Kelly, M. E. (2003). Analysis of edge-detection techniques for crack identification in bridges. *Journal of Computing in Civil Engineering*, 17(4):255–263.
- Argüelles-Fraga, R., Ordóñez, C., García-Cortés, S., and Roca-Pardiñas, J. (2013). Measurement planning for circular cross-section tunnels using terrestrial laser scanning. *Automation in Construction*, 31:1–9.
- Bastien, F., Lamblin, P., Pascanu, R., Bergstra, J., Goodfellow, I., Bergeron, A., Bouchard, N., Warde-Farley, D., and Bengio, Y. (2012). Theano: new features and speed improvements. *arXiv:1211.5590 [cs]*. arXiv: 1211.5590.
- Coleman, T. and Li, Y. (1994). On the convergence of reflective newton methods for large-scale nonlinear minimization subject to bounds vol. 67. *Ithaca, NY, USA: Cornell University*.
- Coleman, T. F. and Li, Y. (1996). An interior trust region approach for nonlinear minimization subject to bounds. *SIAM Journal on optimization*, 6(2):418–445.
- Doulamis, A. (2014). Event-driven video adaptation: A powerful tool for industrial video supervision. *Multimedia Tools and Applications*, 69(2):339–358.
- Doulamis, A. and Matsatsinis, N. (2012). Visual understanding industrial workflows under uncertainty on distributed service oriented architectures. *Future Generation Computer Systems*, 28(3):605–617.
- Fitzpatrick, P., Metta, G., and Natale, L. (2008). Towards long-lived robot genes. *Robotics and Autonomous Systems*, 56(1):29–45.
- German, S., Brilakis, I., and DesRoches, R. (2012). Rapid entropy-based detection and properties measurement of concrete spalling with machine vision for post-earthquake safety assessments. *Advanced Engineering Informatics*, 26(4):846–858.
- Halfawy, M. R. and Hengmeechai, J. (2014). Automated defect detection in sewer closed circuit television images using histograms of oriented gradients and support vector machine. *Automation in Construction*, 38:1–13.
- Han, J.-Y., Guo, J., and Jiang, Y.-S. (2013). Monitoring tunnel deformations by means of multi-epoch dispersed 3d lidar point clouds: An improved approach. *Tunnelling and Underground Space Technology*, 38:385–389.
- Hinton, G. E., Osindero, S., and Teh, Y.-W. (2006). A Fast Learning Algorithm for Deep Belief Nets. *Neural Computation*, 18(7):1527–1554.
- Hinton, G. E. and Salakhutdinov, R. R. (2006). Reducing the Dimensionality of Data with Neural Networks. *Science*, 313(5786):504–507.
- Jahanshahi, M. R., Masri, S. F., Padgett, C. W., and Sukhatme, G. S. (2013). An innovative methodology for detection and quantification of cracks through incorporation of depth perception. *Machine Vision and Applications*, 24(2):227–241.
- Kim, Y.-S. and Haas, C. T. (2000). A model for automation of infrastructure maintenance using representational forms. *Automation in Construction*, 10(1):57–68.
- Koch, C. and Brilakis, I. (2011). Pothole detection in asphalt pavement images. *Advanced Engineering Informatics*, 25(3):507–515.
- Liu, Z., Suandi, S. A., Ohashi, T., and Ejima, T. (2002). Tunnel crack detection and classification system based on image processing. In *Electronic Imaging 2002*, pages 145–152. International Society for Optics and Photonics.
- Makantasis, K., Protopapadakis, E., Doulamis, A. D., Doulamis, N. D., and Loupos, C. (2015). Deep Convolutional Neural Networks for Efficient Vision Based Tunnel Inspection. Cluj-Napoca, Romania.
- Mohanty, A. and Wang, T. T. (2012). Image mosaicking of a section of a tunnel lining and the detection of cracks through the frequency histogram of connected elements concept. volume 8335, pages 83351P–83351P–9.

- Monserrat, O. and Crosetto, M. (2008). Deformation measurement using terrestrial laser scanning data and least squares 3d surface matching. *ISPRS Journal of Photogrammetry and Remote Sensing*, 63(1):142–154.
- Nuttens, T., Stal, C., De Backer, H., Schotte, K., Van Bogaert, P., and De Wulf, A. (2014). Methodology for the ovalization monitoring of newly built circular train tunnels based on laser scanning: Liefkenshoek rail link (belgium). *Automation in Construction*, 43:1–9.
- Pejić, M. (2013). Design and optimisation of laser scanning for tunnels geometry inspection. *Tunnelling and Underground Space Technology*, 37:199–206.
- Protopapadakis, E. and Doulamis, N. (2015). Image Based Approaches for Tunnels Defects Recognition via Robotic Inspectors. In Bebis, G., Boyle, R., Parvin, B., Koracin, D., Pavlidis, I., Feris, R., McGraw, T., Elendt, M., Kopper, R., Ragan, E., Ye, Z., and Weber, G., editors, *Advances in Visual Computing*, number 9474 in Lecture Notes in Computer Science, pages 706–716. Springer International Publishing. DOI: 10.1007/978-3-319-27857-5_63.
- Pynn, J., Wright, A., and Lodge, R. (1999). Automatic identification of cracks in road surfaces. In *Image Processing and Its Applications, 1999. Seventh International Conference on (Conf. Publ. No. 465)*, volume 2, pages 671–675 vol.2.
- Sinha, S. K. and Fieguth, P. W. (2006). Automated detection of cracks in buried concrete pipe images. *Automation in Construction*, 15(1):58–72.
- Son, H., Kim, C., and Kim, C. (2012). Automated Color ModelBased Concrete Detection in Construction-Site Images by Using Machine Learning Algorithms. *Journal of Computing in Civil Engineering*, 26(3):421–433.
- Tung, P.-C., Hwang, Y.-R., and Wu, M.-C. (2002). The development of a mobile manipulator imaging system for bridge crack inspection. *Automation in Construction*, 11(6):717–729.
- Yu, S.-N., Jang, J.-H., and Han, C.-S. (2007). Auto inspection system using a mobile robot for detecting concrete cracks in a tunnel. *Automation in Construction*, 16(3):255–261.